

Ozone generation over the Indian Ocean during the South African biomass-burning period: case study of October 1992.

F. G. Taupin^{1,2}, M. Beekmann³, P. J. Brémaud¹, and T. Randriambelo¹

¹Laboratoire de physique de l'atmosphère, Université de la Réunion, 97715 Saint-Denis messag cedex 9, France

²Now at LPCE-CNRS, 45071 Orléans cedex 2, France

³Service d'Aéronomie du CNRS, Université Pierre et Marie Curie, Paris, 75252 Paris Cedex 05, France

Received: 23 September 1999 – Revised: 19 July 2001 – Accepted: 29 August 2001

Abstract. In this study, we present an estimation of photochemical ozone production during free tropospheric transport between the African biomass burning area and Reunion Island (Indian Ocean) by means of trajectory-chemistry model calculations. Indeed, enhanced ozone concentrations (80–100 ppbv) between 5 and 8 km height over Reunion Island are encountered during September–October when African biomass burning is active. The measurements performed during flight 10 of the TRACE-A campaign (October 6, 1992) have been used to initialise the lagrangian trajectory-chemistry model and several chemical forward trajectories, which reach the area of Reunion Island some days later, are calculated. We show that the ozone burden already present in the middle and upper troposphere over Southern Africa, formed from biomass burning emissions, is further enhanced by photochemical production over the Indian Ocean at the rate of 2.5–3 ppbv/day. The paper presents sensitivity studies of how these photochemical ozone production rates depend on initial conditions. The rates are also compared to those obtained by other studies over the Atlantic Ocean. The importance of our results for the regional ozone budget over the Indian Ocean is briefly discussed.

Key words. Atmospheric composition and structure (evolution of the atmosphere; troposphere – composition and chemistry); meteorology and atmospheric dynamics (tropical meteorology)

1 Introduction

Photochemical ozone production, from biomass burning emissions over Africa during the September–November period, affects large parts of the Southern tropical Indian Ocean as can be seen in TOMS/SBUV daily tropospheric ozone maps (Fishman et al., 1996a). Also, ozone concentrations that we currently measure over Reunion Island during the biomass burning season are about 80–100 ppbv at 5–8 km

height while the background concentrations are about 50–60 ppbv (Taupin et al., 1999). Backtrajectory analyses from locations of enhanced ozone concentrations have shown an origin over southeastern Africa and Madagascar (Baldy et al., 1996; Diab et al., 1996). The forward trajectory analyses of Thompson et al. (1996) from fire locations in southern Africa showed that Reunion Island was within the sphere of influence of southern African biomass burning products. For the period of the TRACE-A campaign (September–October 1992), Garstang et al. (1996) have shown that, south of 18° S, the easterly transport mode out to the Indian Ocean comprised 90% of the transport pathways compared with only 4% out to the west. More recently, Randriambelo et al. (2000) presented a detailed climatological investigation of 7 years (1992–1999) of 2-monthly PTU-O₃ radiosondes. The ozone contamination from biomass burning was shown to be maximum over Reunion Island during October. However, it is not clear (Baldy et al., 1996) whether the ozone build-up is confined to a region near emission sources, with subsequent transport to Reunion Island (Cook-then-Mix), or whether photochemical ozone production is still active over the Indian Ocean (Mix-then-Cook). Therefore, in the present study, we wish to perform trajectory-chemistry modelling in order:

1. to explain the possible photochemical origin of ozone enriched layers observed at Reunion Island and
2. to test, respectively, the validity of the Mix-then-Cook or Cook-then-Mix hypotheses.

The TRACE-A (Transport and Atmospheric Chemistry near the Equator–Atlantic) campaign was conducted in October 1992, to study the source and transport of primary and secondary ozone precursors associated with biomass burning in South America and Southern Africa. The measurements conducted during this campaign have shown that the presence of widespread biomass burning, in both South America and southern Africa, is a primary driver of the “global smog” phenomenon observed in the southern tropics. How-

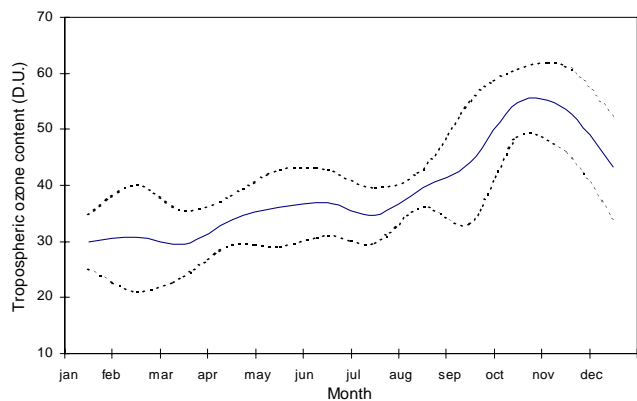


Fig. 1. Seasonal variation of monthly averaged integrated ozone content (thick line) between the ground and the tropopause. The standard deviation calculated from all the 73 profiles is also represented as dashed lines.

ever, the presence of biomass burning is not sufficient to generate the ozone maximum observed far away from the trace gas source; relatively small scale convective processes occurring on each continent collectively become a necessary contributor to the large-scale observed ozone enhancement (Fishman et al., 1996b).

In this paper, we present a case study of the quantification of the ozone generation during the free tropospheric transport between the African biomass burning area and the Indian Ocean, in order to further explain enhanced ozone data observed at Reunion Island which are presented in Sect. 2.1. The simulations have been conducted by using a simple trajectory-chemistry model that we initialise with airborne trace gas measurements made during the TRACE-A experiment conducted in October 1992 over Africa (Fishman et al., 1996b) and presented in Sect. 2.2. The meteorological context of the case study is outlined briefly in Sect. 3. The model is described in Sect. 4. In Sect. 5, the net ozone production between Africa and Reunion Island is calculated and compared to results from other studies. The relevance of the results obtained for larger scale ozone formation from biomass burning and its transport over the Indian Ocean is then discussed.

2 Experimental data and eastward transport from the African continent

2.1 Tropospheric ozone above Reunion Island

The monthly average from 1992 to 1997 of the seasonal variation of column-integrated tropospheric ozone is presented in Fig. 1 (Taupin, 1998; Taupin et al., 1999). The high amplitude of the seasonal variation (25 DU; one Dobson unit equals 2.6×10^{16} molecules/cm²) is due primarily to the high peak (55DU) appearing in October. Several significant influences on ozone concentration above the south-western Indian Ocean have been highlighted and qualitatively demonstrated,

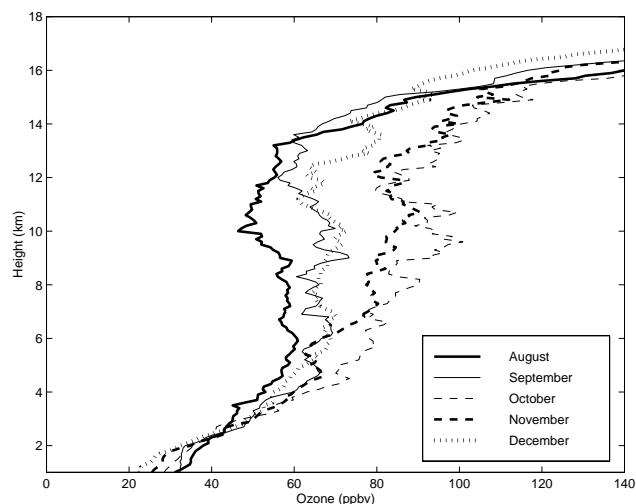


Fig. 2. Mean monthly tropospheric ozone profiles obtained by radiosondes at Reunion Island from August to December (Randriambelo et al., 2000).

namely transport from the stratosphere (Baray et al., 1998), and photochemical formation from biomass burning emissions (Taupin et al., 1999; Randriambelo et al., 2000). In the study of Randriambelo et al. (2000), recent stratospheric intrusions have been eliminated from the ozone climatology using an identification method based on considerations of ozone, humidity, vertical stability and meteorological conditions. Figure 2, extracted from Randriambelo et al. (2000), presents averaged monthly tropospheric ozone profiles obtained by radiosondes at Reunion from August to December 1992 to 1998; these are considered to be representative from the biomass burning source. It clearly shows a maximum of ozone appearing in October that can be explained by the presence of intense fires and of deep convective clouds both in the south-eastern African continent and Madagascar.

In this study, we will focus on the ozone measurements performed at Reunion Island during the same period as three flights of the TRACE-A campaign on the African continent. Indeed, the large number of species measured during this campaign can provide a unique opportunity to best constrain the initial conditions for modelling the ozone formation during transport from the African continent to the Indian Ocean. Two Reunion Island measurement dates are concerned, the 6 and 13 October 1992. The Fig. 3 presents the vertical profiles of relative humidity, temperature and ozone mixing ratio recorded from the surface to 12 km (1000 to 150 hPa) for these two dates.

Regarding the temperature, several thermal inversions can be visually identified in each case. Between each thermal inversion stable layers are capped that correspond to a strong relative humidity decrease and ozone enhancement. The first inversion is localized between 800 and 700 hPa depending on the case study. This corresponds to the well-known trade-inversion (Taupin et al., 1999). The ozone enhancement observed in this stable layer is 10 to 30 ppbv. Above 700 hPa,

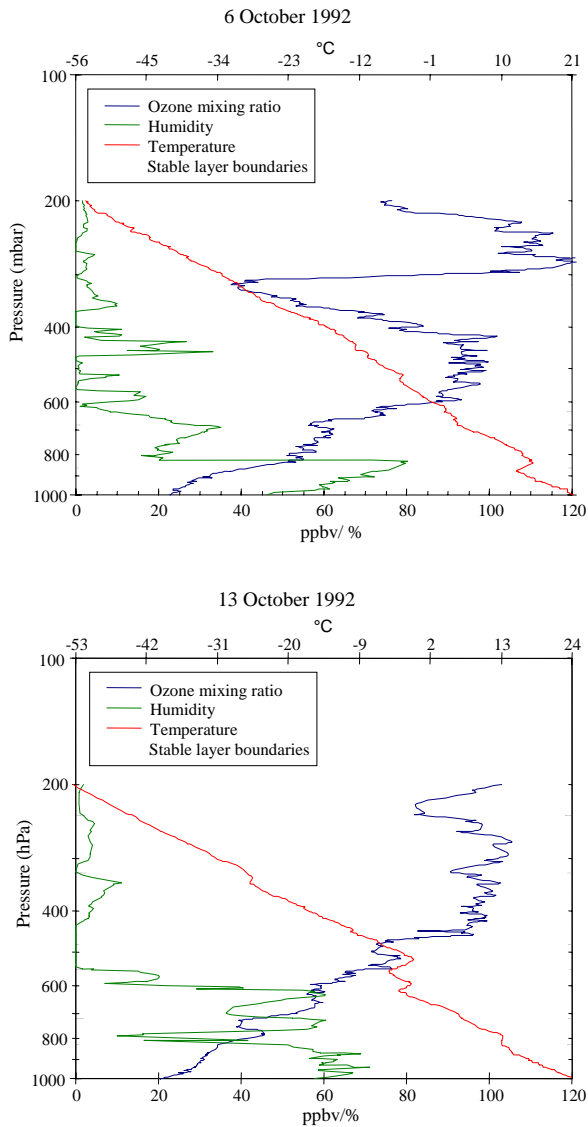


Fig. 3. Altitude profiles of temperature, relative humidity, and ozone mixing ratio measured at Reunion Island for two dates: 6 October (a), and 13 October (b), 1992.

each case study differentiates by the number of stable layers. Concerning the 6 October profiles, one large contaminated layer can be visualized from 680 to 320 hPa. This corresponds to a large ozone enhancement (35 ppbv) which mixing ratio increases up to 95 ppbv. The 13 October 1992 temperature profile is characterized by at least four inversions from 600 to 340 hPa. An ozone enhancement corresponds to each inversion, the larger mixing ratio observed (95 ppbv) is localized from 450 to 340 hPa. Another ozone enhancement is identified above 300 hPa that reaches 100 and 120 ppbv on the 13 and 6 October 1992, respectively. When regarding at ozone concentration (molec/cm^3), the layer localized between 600 and 400 hPa on 6 October 1992, and from 500 hPa to 300 hPa on 13 October 1992 constitutes the ozone maximum for each profile.

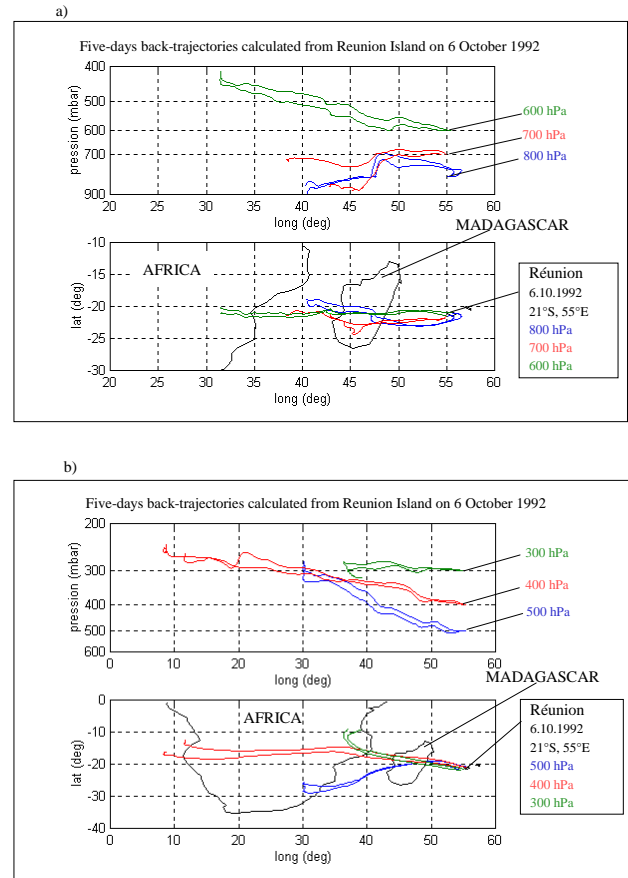


Fig. 4. Five-days backward trajectories ending over Reunion Island the 6 October 1992 for 6 pressure levels. (a) 800 hPa, 700 hPa, and 600 hPa. (b) 500 hPa, 400 hPa, and 300 hPa. The representation is two 2D projections: longitude-latitude in the lower panel, longitude-pressure in the upper panel.

A detailed back-trajectory study has been performed for each case in order to identify the origin of the observed ozone enhancements. Each profile has been separated in six pressure levels: 800, 700, 600, 500, 400 and 300 hPa. The results are shown in Fig. 4 (6 and 5 October (13 October)). A westerly origin from the African continent or Madagascar is identified at all levels for the 6 October 1992, which explains why the troposphere appears rather more homogeneous than on 13 October. Concerning 13 October 1992, the westerly origin from Madagascar or the African continent is present at 700 hPa, 600 hPa, 400 hPa, and 300 hPa. At 500 hPa, the air mass origin is southwest, with a very strong subsidence during the transport (250 hPa between 3 days). Usually, the zonal circulation appears to be from the East, from 800 hPa to 700 hPa during this period (Taupin et al., 1999). When regarding the air mass trajectories performed at 800 hPa (Figs. 4 and 5) in both October 1992 cases, an Easterly origin is definitely observed as the air mass passes over Reunion Island. However, the five-day origin of the air mass appears to become westerly, which signifies

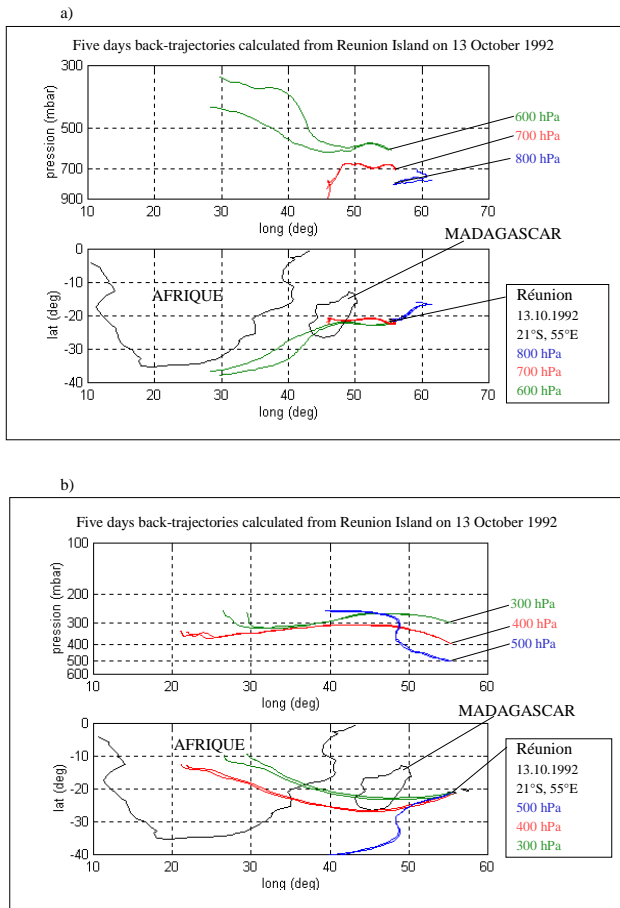


Fig. 5. The same as Fig. 4, but for 13 October 1992.

that a recirculation occurs in the Indian Ocean due to the descending branch of the walker cell. This recirculation allows contamination of the Reunion Island lower troposphere with biomass burning product just above the trade-inversion. One can note the particular 500 hPa back-trajectories calculated for 13 October 1992. Two remarkable points are to be noted concerning this particular case; the southerly origin of the air mass and the strong subsidence during transport (50 hPa/day). This trajectory corresponds to a thin layer of ozone enhancement on the ozone profile (Fig. 3) and dry air on the relative humidity profile. These features constitute similarities between this trajectory case and those already shown by Baray et al. (1998) and described as stratospheric air intrusions. A tracer study, using potential vorticity, would allow in to classify this ozone enhancement as stratospheric in origin.

Unfortunately, no TRACE-A measurements were available for the days of air mass departure from the African continent. Therefore, the aim of the present study is somewhat limited in the sense that it tends to make a link between the chemical evolution of biomass burning emissions and general features in ozone observations above Reunion Island. However, as previously noted, using the data obtained during this campaign provides a unique constraint on the initial

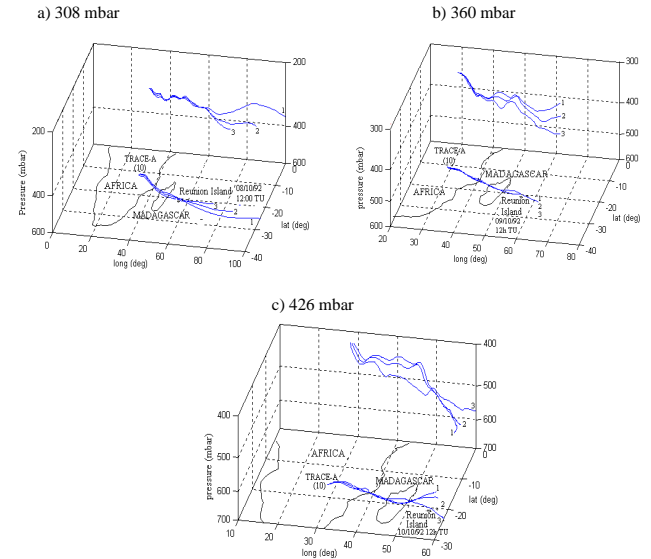


Fig. 6. Forward trajectories calculated from flight 10 of the TRACE-A campaign. The time resolution of computation is 10 min, and use E. C. M. W. F. data. **(a)** 308 hPa, **(b)** 360 hPa, **(c)** 426 hPa. The graph is 3-Dimensionnal: x-axis is latitude, y-axis is longitude, and z-axis is pressure. Two projections of the trajectories have been represented: longitude-pressure and latitude-longitude.

conditions for modelling the ozone formation during transport from the African continent to the Indian Ocean. Consequently, the modelling study will be performed from the TRACE-A campaign toward the Indian Ocean. We will also quantify the ozone production that occurs during the upper tropospheric transport of contaminated air masses and tentatively explain the role of biomass burning in the ozone enhancements observed above Reunion Island.

2.2 TRACE-A data

In order to perform this modelling study, we need measurements to initialise the chemical model box near the African biomass burning source regions. Airborne measurements obtained during the TRACE-A campaign will be used for this purpose. In particular, the upper tropospheric air masses sampled during flight 10 were most strongly affected by biomass burning emissions (Fishman et al., 1996b). In order to analyse which of these polluted air masses could possibly be transported to Reunion Island, eight three-to-six day forward trajectories have been calculated starting at flight positions from 800 to 300 hPa. These kinetic air mass trajectories are calculated from 3D wind fields provided by the European Centre for Medium-range Weather Forecast (ECMWF) analyses at 6 h intervals on a 0.75° grid. The trajectory module delivers, at each time step of 10 min, the instantaneous position, pressure, temperature and humidity to the chemical module (see below). The validity of the trajectory package for its use over the Indian Ocean has been previously demonstrated by Baldy et al. (1996).

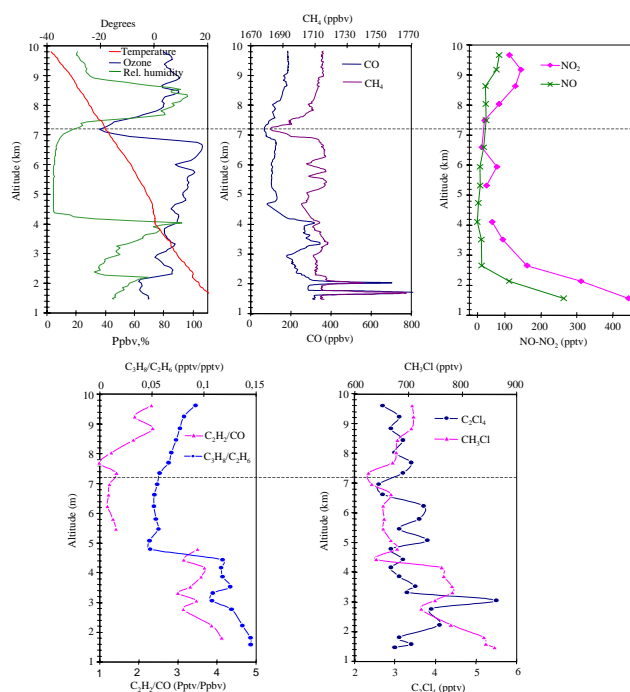


Fig. 7. Chemical data measured during the flight 10 of TRACE-A campaign over a biomass-burning region of Southern Africa. The layer corresponding to the pressure levels 308 hPa and 360 hPa has been delimited (7–10 km).

Table 1. Trace gas concentrations measured in the layer corresponding to the pressure level 426 hPa and used for the initialisation of the trajectory-chemistry model in this case

Component	Measured Values
Ozone (ppbv)	78–81
NO _x (pptv)	115–122
CO (ppbv)	128–140
CH ₃ Cl (pptv)	674
C ₂ Cl ₄ (pptv)	4,1
C ₃ H ₈ /C ₂ H ₆ (pptv/ppbv)	0,07
C ₂ H ₂ /CO (pptv/ppbv)	1,4
Ethene (pptv)	5
Ethane (pptv)	790
HNO ₃ (pptv)	1400

From this study forward trajectories have been selected which indeed pass in the free troposphere over Reunion Island some days later (Fig. 6). These trajectories will be used to study the evolution of ozone and its precursors during transport in the free troposphere over the Indian Ocean. The first two trajectories correspond to the second descent of flight 10; they have been extracted from an upper tropospheric layer ranging from 7 to 9 km and are located at 11°S, 29E, centred in the vertical around 308 hPa and 360 hPa, respectively. The third trajectory corresponds to a longer horizontal flight leg of the aircraft at 426 hPa, near 15°S, 28°E.

The measurements obtained during the second descent of

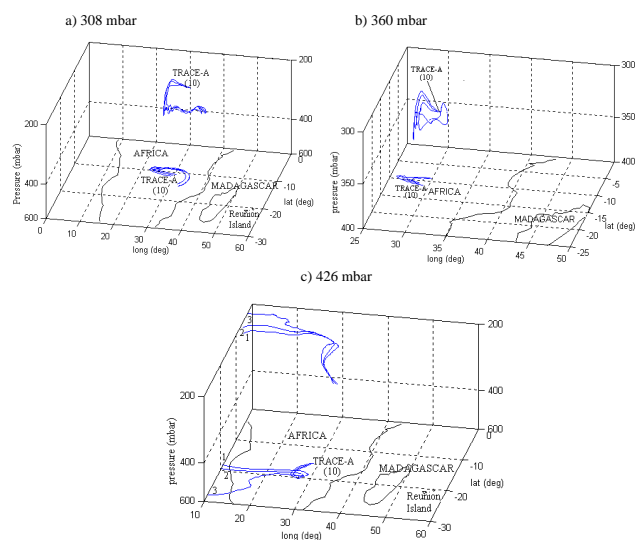


Fig. 8. Same as Fig. 6, but backward instead of forward trajectories.

flight 10 are presented in Fig. 7; the chemical characteristics of the layer centred on the 426 hPa pressure level are shown in Table 1. The ratios C₃H₈/C₂H₆ and C₂H₂/CO have been calculated from the measurements, in order to roughly estimate the age of the air mass relative to a contamination by a pollution event, following a method developed by (Gregory et al., 1996) (relative chemical age).

The relative chemical age of the layers at 308 and 360 hPa is estimated to be 3–5 days (Fig. 7). The layer containing the pressure level 426 hPa has aged by more than 5 days (Table 1). More recent contact with emissions by layers at 308 and 360 hPa also tends to be confirmed by the abundance of ethylene, a short lifetime hydrocarbon whose mixing ratios are equal to 20 pptv at 308 and 360 pptv against 5 pptv at 426 hPa in the third layer. Measured mixing ratios of CH₃Cl (Fig. 7), a specific tracer for biomass burning (Gregory et al., 1996), show a sensitive increase (from 600 to 670–700 pptv) in all three layers studied as compared to the altitude range located just below (4–6 km), suggesting biomass burning as the origin of the contamination. On the contrary, the mixing ratios of C₂Cl₄, a tracer for urban pollution, are always low. Finally, the large relative humidity values recorded from 400 to 300 hPa tend to favour recent contamination by a convective event, that could explain a biomass burning contamination in the upper troposphere.

In addition, to best identify the origin of the air masses studied, we have also calculated four to five day back-trajectory clusters (central trajectory plus four trajectories shifted by ±1° in longitude and latitude) for all three pressure levels (Fig. 8). The five-day origin of the air mass arriving at 308 hPa is near the East coast of the African continent (Fig. 8a), where biomass burning is very active during this period as shown by Randriambelo et al. (1998) and illustrated on Fig. 9. In addition, these trajectories display strong ascendant motion (pressure decrease by about 100 hPa) 30 h before arriving when travelling through a convective region (Fig. 9).

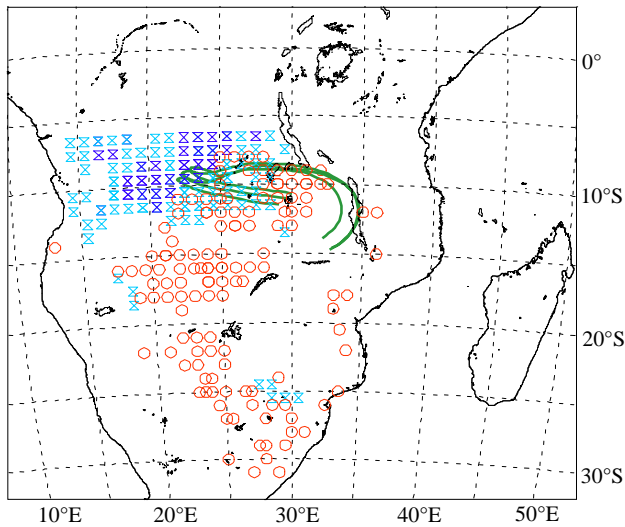


Fig. 9. Map of the southwestern Indian Ocean region, showing TOVS (<http://eosdata.gsfc.nasa.gov>) cloud top height and precipitations values extracted for the 4 and 5 October 1992. The locations where the cloud top height is higher than 320 mbar, and precipitations larger than 7 mm/day are shown in light blue, locations with cloud top height above 320 hPa and precipitations larger than 15 mm/day are dark-blue drawn. The locations of intense fires have been added for the 3–4 October period with red circles. The back trajectories cluster, calculated from TRACE-A measurement locations at 308 hPa the 6 October 1992, and described in Fig. 6 is also shown.

This region has also been identified as a strong to deep convection zone (cloud top height from 7–10 km to tropopause) by Thompson et al. (1996) and well schematised by Jacob et al. (1996) using the Walker circulation. Also the air mass at 360 hPa (Fig. 8b) originates over the eastern coast of the African continent.

Thus, from all these arguments (trace gas ratios, biomass burning tracers, fire and convection locations, trajectories), a contamination of the layers at 308 and 360 hPa with African biomass burning emissions seems very probable.

On the contrary, the back trajectory for the third layer (426 hPa, Fig. 5c) indicates an origin of the air mass over the Atlantic Ocean, without contamination during the last five days, that agrees well with a 5 to 6 day relative chemical age. The ozone mixing-ratio is larger than 75 ppbv in all layers; thus significant ozone build-up has already occurred between the time of emission and measurement. However, as NO_x mixing ratios mostly exceed 100 pptv and the CO mixing ratios exceed 100 ppbv, further net photochemical ozone formation may be expected to occur over the Indian Ocean.

3 Meteorological context of the TRACE-A period

Figure 10 shows the ECMWF analysed wind fields at 1000 and 500 hPa for 6 October 1992, the first day of our trajectory-chemistry study. At the 1000 hPa level, winds

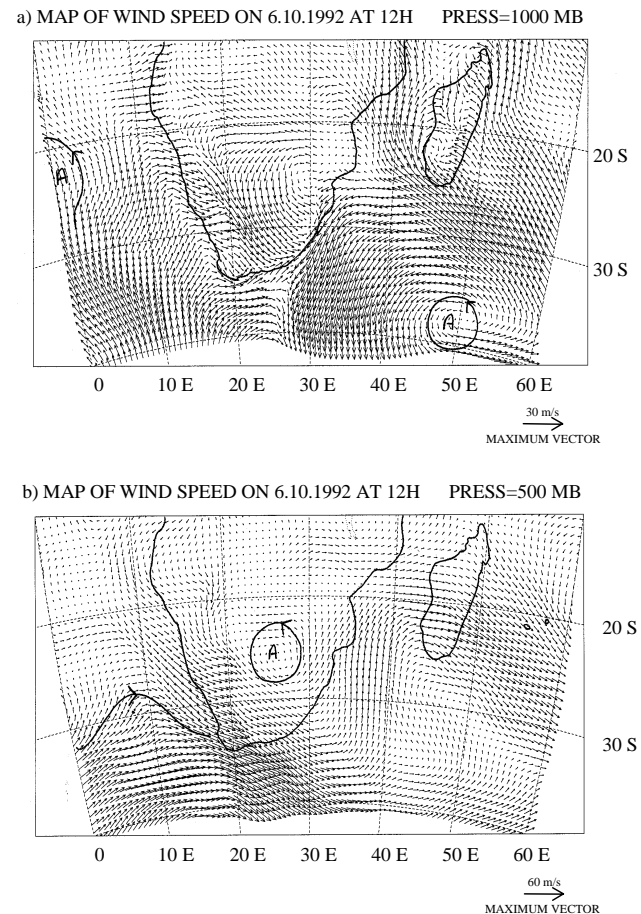


Fig. 10. Meteorological context of the TRACE-A campaign. Horizontal wind on isobaric surfaces on 6 October 1992, at 12:00 T. U., from ECMWF data. a) Surface, b) 500 hPa.

are weak and variable over Southern Africa north of 20°S. South of 20°S, winds over Southern Africa are confluent and deviated to a southerly direction. The mid-troposphere at 500 mbar (approximately 5.5 km, Fig. 10b) is characterised by the predominance of the westerly flow over the Indian Ocean. At upper levels (200 hPa, not shown), we note a prevailing zonal flow from West to East in the whole region. The circulation patterns observed on 6 October 1992 are generally representative of the whole TRACE-A period (from 21 September to 27 October 1992) (Bachmeier et al., 1996). This allows us to consider the particular period studied here as rather typical for free tropospheric long-range transport of biomass burning emissions and products.

4 Model description

The trajectory-chemistry model used for this work describes the evolution of chemically active species of an air parcel during its transport along a trajectory. It is the free tropospheric version of the trajectory-chemistry model MELCHIOR (Modèle Lagrangien de CHimie de l'Ozone à l'échelle Régionale) developed at Service d'Aéronomie for

studies in the boundary layer (Lattuati, 1997). The free tropospheric model consists of three parts:

1. the calculation of air mass trajectories,
2. the chemical initialisation of the air parcel, and
3. the calculation of the chemical evolution of the species.

The advantages of the use of a lagrangian model in this study are its simple set-up and the fact that individual air parcels can be studied. This makes the model initialisation straightforward and allows a more direct interpretation of the results as compared to a 3D eulerian model study.

The air mass trajectories used by the lagrangian model are those previously used (Fig. 3) to demonstrate the free tropospheric transport of air masses between the African biomass burning zones and Reunion Island. The gas phase chemical reaction scheme used in the chemistry module describes the chemical behaviour of 77 gaseous species, through about 150 reactions (Lattuati, 1997). This scheme has been extended and updated from an original continental boundary layer chemistry scheme (Hov, 1985). The hydrocarbon degradation scheme is very similar to the EMEP gas phase chemical mechanism (Simpson, 1992) and is a priori adapted as for biomass burning as well for industrial or traffic emissions. Six hydrocarbon species (ethane, butane, ethene, propene, isoprene and *o*-xylene) represent alkane, alkene, ketones and aromatic compounds. Their oxidation by OH, O₃ and NO₃ yields eleven oxygenated compounds, including formaldehyde and higher aldehydes, ketones, bicarbonyls, unsaturated carbonyls and alcohols. Adaptations have been made to allow the simulation of free tropospheric conditions. In particular, pernitrates (HNO₄, CH₃NO₄) have been added and the pressure dependence of three body reactions has been included (Troe reactions). RO₂ and RO₂ recombination reactions, which may be important for the degradation of VOC emissions in low NO_x environment, have also been explicitly taken into account. All rate constants have been updated from Atkinson (1994).

Photolysis frequencies *J* are calculated using a simple relationship with the zenith angle ζ ($J = A \cdot \exp(-B/\cos\zeta)$). *A* and *B* factors are taken from a look-up table which has been previously set-up for different altitudes, total ozone columns and cloud cover scenarios (Flatoy et al., 1996) by using the radiative transfer model of Jonson and Isaksen (1993). For this study, a total ozone column of 297 DU is used consistent with measurements from TOMS data and ozone sounding performed at Reunion Island (Taupin, 1998). Cloud free conditions are assumed to prevail during this study, which has been shown from satellite pictures (Fuelberg et al., 1996; Bachmeier et al., 1996).

The air mass trajectories are chemically initialised with aircraft measurements (see also Sect. 3). Measured VOC's, not represented in the gas phase mechanism are replaced by one of the six hydrocarbons and 11 oxygenated hydrocarbons included in the code with the most similar structure and reactivity. In particular, acetone and acetylene measured during

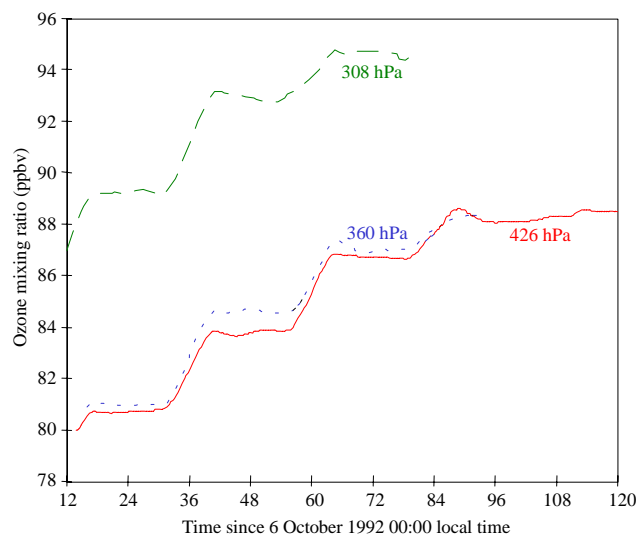


Fig. 11. Ozone generation simulated for 6–10 October 1992, during transport from TRACE-A flight position to Reunion Island.

the TRACE-A campaign are represented by ethane and the propane has been replaced by *n*-butane. The aromatic compounds chemistry (here benzene and toluene) has been represented by the *o*-xylene chemical scheme. Mass weighting and a reactivity-weighting factor following the procedure of Middleton et al. (1990) is applied. Nevertheless, in Sect. 4.2, it will be shown that the exact knowledge of the NMHC distribution is not critical for the calculation of net ozone production rates.

5 Results and discussion

5.1 Ozone production between Africa and Reunion Island

The chemical box of the trajectory-chemistry model described in Sect. 3 has been run along the forward trajectories calculated from flight 10 and ending over Reunion Island (Fig. 7). The trajectories keep their homogeneity until they arrive over Reunion Island about three to four days later. In addition, we note a strong subsidence on each calculated trajectory. The trajectory cluster, calculated from 308 hPa over Africa, reaches Reunion Island two and a half days later at 371 hPa, with a subsidence rate of 25 hPa/day. The second cluster, starting at 360 hPa, arrives over Reunion Island three days later at 471 hPa, corresponding to a subsidence rate of 37 hPa/day. The third cluster, calculated from the pressure level 426 hPa, reaches Reunion Island 4 days later at 521 hPa; the subsidence rate is 24 hPa/day. The subsidence motion indicates that the atmosphere is stratified and that vertical mixing should be weak; hence the lagrangian approach is justified in these cases. When regarding the ozone profile measured at Reunion Island during this period, the ending levels of the trajectories fall in the layer of ozone maximum concentration recorded (not shown).

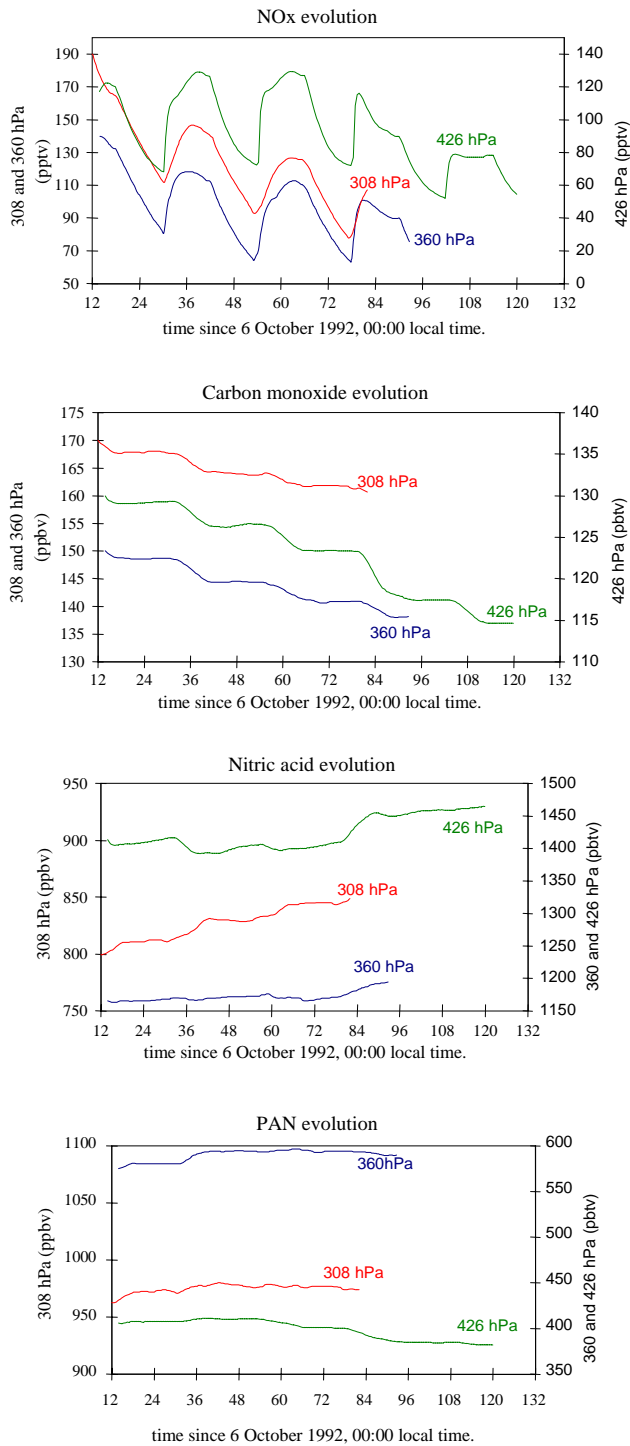


Fig. 12. As Fig. 8, but for NO_x, CO, HNO₃ and PAN.

The evolution of the ozone mixing-ratio for each trajectory studied is presented in Fig. 11. The main result is that ozone production during transport to Reunion Island, at all pressure levels studied, is still significant, declining from 3–4 ppbv/day for the first day to 1–2 ppbv/day for the subsequent days. On the average, we obtain a net ozone production rate between 2.5 and 3 ppbv/day during transport from

the African continent to Reunion Island. This ozone production rate appears to be rather homogeneous, which is explained by the fact that initial concentrations for ozone precursors are comparable (140–190 pptv NO_x, ~2 ppb NO_y, 150–170 ppbv CO). The sensitivity of ozone production rates with respect to initial conditions will be analysed in more detail in Sect. 5.2.

Also, the chemical evolution of some other important trace gases is similar for the three air masses studied (Fig. 12). NO_x species are consumed during transport and transformed into reservoir species HNO₃ and PAN. This corresponds to the largest ozone production on the first day of the simulation and to the lower rates on subsequent days. NO_x concentrations on the third day at noon are, respectively, 110, 95 and 100 pptv for the trajectories starting at 308, 360 and 426 hPa, which is still enough to support net photochemical ozone production. Conversely, reservoir species HNO₃ and PAN slightly increase during the simulation, with the exception of PAN for the trajectory at 426 hPa. The carbon monoxide net destruction varies between 3 ppbv/day and 6 ppbv/day which implies that, roughly, between half (for trajectories starting at 308 hPa and at 426 hPa) and one ozone molecule (trajectory 2) are formed per one CO molecule consumed.

We now compare the ozone production rates obtained in our study with other studies. From observations of the ozone content integrated between 1.5 and 7 km, Gregory et al. (1996) studied the effects of ageing as African air moves off the West African coast over the Atlantic Ocean. By comparing two measured profiles separated by two days of transport, these authors derive a net photochemical ozone production of 6 ppbv/d during transport. Differences with our lower value may be attributed to four reasons,

1. the different region considered (South Atlantic basin vs. Indian ocean),
2. the lower height range in the Gregory et al. 1996 study (1.5–7 km compared to about 5–9 km in our study),
3. the uncertainty inherent in ozone production rates from small differences between ozone profiles, and
4. the uncertainty in the same estimations from photochemical models (see discussion in Sect. 5.3).

By means of a photochemical model (Jacob et al., 1996) have conducted simulations of the instantaneous net ozone production, scaled to a diurnal average, using all measurements performed during the TRACE-A period. This approach is similar to ours but note that our net ozone production rates are calculated by taking into account the decline of ozone precursors and in particular NO_x during the days after the measurements, whereas Jacob et al. (1996) assumed the O₃ precursors to be constant, except NO, over the calculation period. Near source regions of emission, over the Southern African continent and near its eastern coast Jacob et al. (1996) estimate for the 8 to 12 km range a net ozone production per day between 1 to about 18 ppbv, with most of the values around 2–4 ppbv/day. Over the South Atlantic

Table 2. Sensitivity of ozone production to modifications in the initial concentrations of some important compounds for the chemical trajectory starting at 308 hPa. Results are presented as percentage change with respect to the net ozone production obtained in the reference case

Initial concentration changes	% Change on ozone production	
NMHCs	+30%	-2.6
	-30%	+2.1
CO	+30%	+7.5
	-30%	-9.5
NO _x	+30%	+17.2
	-30%	-20.7
HNO ₃	+30%	+8.2
	-30%	-8.7
H ₂ O	+30%	+1.6
	-30%	-2.6

basin, that is several days of transport away from the probable source regions, they still estimate a net photochemical ozone production of 2.1 ppb/day in the 8–12 km range and less than 2 ppbv/day in the 4–8 km range. These values are similar to our estimations in the 5–9 km altitude range of about 2.5–3 ppbv/day on the first day (near source regions) and 1–2 ppbv/day after several days of transport. This means that photochemical ozone production over the Indian ocean is probably of the same order of magnitude of as that calculated over the south Atlantic basin.

5.2 Influence of initial concentrations on ozone production

In this section, we study the sensibility of net ozone production with respect to initial concentrations of several species in order to study the chemical regime of the biomass burning plume and also to encounter the effect of the uncertainty inherent in the initial conditions employed. For example, real NMHC's are represented by model species sometimes with different reaction paths (for example acetylene and acetone represented by ethane). Moreover, NO₂ concentrations measured during the TRACE-A campaign have been estimated to be rather uncertain (Jacob et al., 1996). Finally, nitric acid measurements are sparse (2–15 min time resolution compared to 3 min for NO) (Jacob et al., 1996); so each measured data corresponds to a larger altitude range than considered for the initialisation of each air parcel. In order to study the sensitivity of ozone production, with respect to these compounds and also to other chemically important species such as CO and water vapour, we have applied a 30% variation to the initial concentrations for the trajectory at 308 hPa. The 30% value is not meant to represent the uncertainty of any of these initial concentrations; it is merely chosen to provide a common basis for the comparison of the sensitivities.

The results summarised in Table 2 indicate the strongest sensitivity of NO_x initial concentrations. Indeed, ozone production is basically NO_x limited. Also, the sensitivity of

nitric acid initial concentration is important as HNO₃ photolysis is an important pathway for NO_x recycling. CO is important also as it transforms OH into HO₂, which reduces removal of NO_x by OH. On the other hand, water vapour concentrations are not very sensitive; apparently the availability of OH and subsequently HO₂ and RO₂ radicals from the reaction of O(¹D) with water vapour does not much effect the net ozone production. Surprisingly, the sensitivity of NMHC initial concentrations is slightly negative. The reason for this is that, first, the largest contribution to OH to HO₂ conversions stems from CO and, second, an increase in NMHC's favours PAN formation which consumes NO_x and thus decreases ozone production.

This study suggests that the strongest uncertainty on the calculated net ozone production rate probably stems from the uncertainty in NO_x measurements. Indeed, some disagreements have been found between measured and simulated NO₂/NO ratios (Smyth et al., 1996) that we have also observed. Moreover, the determination of NO₂ was often at or below the instrument's limit of detection during the TRACE A campaign and may include contributions from HO₂NO₂ or N₂O₅ (Smyth et al., 1996; Sandholm et al., 1994). Since we have used the measured NO_x values (NO + NO₂), we will consider them as an upper limit.

5.3 Larger scale relevance of the results

We will now briefly discuss the representativity and the larger scale importance of our results. To this purpose, and as it represents the layer with the largest ozone production among the studied cases (3 ppbv/day), we have compared the initial concentrations used for the trajectory starting at 308 hPa with average mixing ratios measured during the TRACE-A flight 10 at similar altitudes. This layer around 308 hPa is one of the most polluted sampled at this altitude and during this flight (see Table 3). In addition, as previously discussed, the measured NO_x concentrations have to be considered as upper limits. Thus, our value of a 2.5–3 ppbv/day net ozone production probably represents an upper limit for more average conditions over the Western Indian Ocean during October.

Also, we may ask, what will be the chemical evolution of the air mass when transported further westward from Reunion Island, over the Indian Ocean. A longer-term simulation of the layer at 308 hPa (not shown) shows that, on day 6, the NO_x mixing ratio approaches its steady state concentration where loss reactions are balanced by a supply of fresh NO_x from reservoir species HNO₃ and PAN. This corresponds to daily maximum NO concentrations of about 30 pptv, allowing no further net ozone production but preventing ozone loss. The maps of tropospheric ozone content derived from satellite analyses presented by Fishman et al. (1996a), show that the maximum of ozone increase is reached not far eastward from Reunion Island, as predicted by our study. The satellite analysis also shows a large eastward extension of the plume (at least to 60° E, the limit of the analysed domain), again in line with our finding of a

Table 3. Main mixing ratios measured during flight 10 of the TRACE-A campaign around the 308 hPa pressure level, as compared with the initial mixing ratios used to initialise the same level simulation

Species	Modelled initial mixing ratios	Flight 10 Measurements	
		Min-max	Number of soundings
NO _x	191 pptv	84–210 pptv	18
HNO ₃	800 pptv	689–1256 pptv	3
PAN	963 pptv	594–963 pptv	3
Ozone	87 ppbv	80–90 ppbv	70
CO	170 ppbv	68–79 ppbv	100
CH ₄	1713 ppbv	1623–1723 ppbv	100
NMHCs	1537 pptv	458–1609 pptv	15

near zero photochemical ozone balance after about a week of transport and thus a very large lifetime of ozone in the upper troposphere over the Indian ocean.

At this stage of plume ageing, and in the absence of a fresh supply of NO_x sources, for example, from lightning (Smyth et al., 1996), it is the dilution or heterogeneous removal of the NO_x reservoir species which will ultimately drive the lifetime of the large ozone burden produced from biomass burning emissions and its impact on the global tropospheric ozone budget. After several days of transport, the hypothesis of no mixing of the air parcels made for these calculations becomes more and more questionable. However some hypotheses can be driven that are linked to the walker cell circulation:

As the air subsides over the Indian Ocean (Fig. 6), net ozone loss can take place in the lower troposphere. The air masses then reach the Easterly circulation (descending branch of the walker cell) and bring residual ozone produced from biomass burning emissions in Reunion Island lower troposphere, just above the trade-inversion (Fig. 3). This hypothesis can be corroborated with the presence of two ozone concentration (when converting the mixing ratio into molec/cm₃) maxima located just above the zonal wind inversion for the larger one, and between the trade-inversion and the zonal inversion for the second one.

In view of the current findings, one can wonder what is then the role of biomass burning on tropospheric ozone concentration over Reunion Island as compared with stratospheric intrusion. Ozone produced from biomass burning emissions is displayed in the whole troposphere above the trade-inversion over Reunion Island from August to December. Stratospheric intrusions occur at different altitudes over Reunion Island by way of tropopause breaks due to the westerly Jet-stream (Baray et al., 1998) during winter, and near zones of deep convection during summertime (Baray et al., 1999). These events are very strong (up to 200 ppbv of ozone) but time limited (few days); ozone decrease takes place rapidly due to low NO_x mixing ratios conditions, and to subsidence. At present, biomass burning constitutes the main source of ozone in the Mid to upper-troposphere of Reunion island.

We can also compare the contamination that occurs over

the Indian Ocean with the contamination of the South Atlantic basin. Even if the production rates of ozone in the free troposphere are comparable, the tropospheric ozone content appears to be larger above Ascension Island, for example (Fishman et al., 1996). Indeed, the Atlantic basin troposphere is contaminated by both the American continent and the African continent. The Indian Ocean free troposphere is primarily contaminated by the African continent and secondarily by Madagascar; the lower troposphere, above the trade-inversion at Reunion Island, also appears to be contaminated due to the recirculation of the upper troposphere air masses over the Indian Ocean due to the descending branch of the Walker cell; this does not constitute a fresh source of biomass burning products.

6 Conclusion

This paper presents a case study of ozone production over the Indian Ocean during the African biomass-burning period. To this purpose, we use a trajectory-chemistry model driven by ECMWF analyses and initialised by TRACE-A data. We show that the net upper tropospheric ozone production between the Southern African East coast and Reunion Island is about 2.5–3 ppbv/day for the three trajectories studied which corresponded to the most polluted upper tropospheric layers of TRACE-A flight 10. Our result also falls in the range of values calculated by Jacob et al. (1996) from all TRACE A data between 4 and 12 km, although Jacob et al. (1996) calculate net ozone production rates with fixed precursor concentrations whereas our study allows for decay of precursors. Indeed, our study has shown that a 30% difference in the initial NMHC concentrations does not sensibly change the averaged net ozone production rate. Consequently, this sensitivity study, with varying initial concentrations, reveals that our calculated net ozone production is most sensitive to the uncertainty in NO_x concentrations used for initialisation and also to HNO₃, supplying fresh NO_x and CO, but is only a little sensitive to NMHC initial concentrations and to water vapour. This result shows that the Reunion Island free troposphere (higher than 3 km) is mostly contaminated by ozone produced near emission sources (Cook-then-Mix), with little enhancement during transport (less than 10%). Our results

also explain the maximum in the ozone plume observed from satellite data near Reunion Island (Fishman et al., 1996a) and its large eastward extension over the Indian Ocean. However, several factors are simultaneously needed that contribute to the ozone enhancement observed over Reunion Island: High ozone concentrations observed in the troposphere over Reunion Island are primarily due to biomass burning that occurs on the African continent and Madagascar. The intensity of the ozone peaks observed depends on the intensity of the fires and of the deep convection occurring not far from the source zones. The variability of the ozone mixing ratios with altitude depends on the zonal circulation, i.e. the westerlies in the free troposphere (higher than 5 km), and the presence of recirculation on the Indian Ocean with the descending branch of the walker cell.

Acknowledgement. We wish to thank Y. Pointin, and A. M. Lanquette (LaMP, Clermont-Ferrand, France) for supplying the analysis software of ECMWF data, as well as the TRACE-A Science Team for providing access to the data obtained during the GTE TRACE-a Field Mission on a data archive (<http://www-gte.larc.nasa.gov>).

Topical Editor D. Murtagh thanks two referees for their help in evaluating this paper.

References

- Atkinson, R.: Gas phase tropospheric chemistry of organic compounds, *J. Phys. Chem. Ref. Data, Monograph 2*, 1994.
- Bachmeier, A. S. and Fuelberg, H. E.: A meteorological overview of the TRACE-A period, *J. Geophys. Res.*, 101 (D19), 23 881–23 888, 1996.
- Baldy, S., Ancellet, G., Bessafi, M., Badr A., and Lan-Sun-Luk, J. D.: Field observations of the vertical distribution of tropospheric ozone at the island of Reunion (southern tropics), *J. Geophys. Res.*, 101 (D19), 23 835–23 850, 1996.
- Baray, J. L., Ancellet, G., Taupin, F. G., Bessafi, M., Baldy, S., and Keckhut, P.: Subtropical tropopause break as a possible stratospheric source of ozone in the tropical troposphere, *J. Atm. Sol.-Terrestr. Phys.*, 60 (1), 27–36, 1998.
- Baray, J. L., Ancellet, G., Randriambelo T., and Baldy, S.: Tropical cyclone Marlene and stratosphere-troposphere exchange, *J. Geophys. Res.*, 104 (D11), 13 953–13 970, 1999.
- Diab, R. D., Jury, M. R., Combrink, J. M., and Sokolic, F.: A comparison of anticyclone and trough influences on the vertical distribution of ozone and meteorological conditions during SAFARI-92, *J. Geophys. Res.*, 101 (D19), 23 809–23 822, 1996.
- Fishman, J., Brackett, V. G., Browell E. V., and Grant, W. B.: Tropospheric ozone derived from TOMS/SBUV measurements during TRACE-A, *J. Geophys. Res.*, 101 (D19), 24 069–24 082, 1996a.
- Fishman, J., Hoell, Jr., J. M., Bendura, R. D., Mc Neal, R. J., and Kirchoff, V. W. J. H.: NASA GTE TRACE A Experiment (September–October 1992): Overview, *J. Geophys. Res.*, 101 (D19), 23 865–23 880, 1996b.
- Flatoy, F., Hov, O., and Smit H. G. J.: Three dimensional model studies of exchange processes of ozone in the troposphere over Europe, *J. Geophys. Res.*, 100 (D6), 11 465–11 481, 1995.
- Fuelberg, H. E., Loring, Jr., R. O., Watson, M. V., Sinha, M. C., Pickering, K. E., Thompson, A. M., Sachse, G. W., Blake, D. R., and Schoerberl, M. R.: TRACE A trajectory intercomparison, 2, Isentropic and kinematic methods, *J. Geophys. Res.*, 101 (D19), 23 927–23 940, 1996.
- Garstang, M., Tyson, P. D., Swap, R., Edwards, M., Källberg, P., and Lindesay, J. A.: Horizontal and vertical transport of air over southern Africa, *J. Geophys. Res.*, 101 (D19), 23 721–23 736, 1996.
- Gregory, G. L., Fuelberg, H. E., Longmore, S. F., Anderson, B. E., Collins, J. E., and Blake, D. R.: Chemical characteristics of tropospheric air over the tropical south Atlantic Ocean: Relationship to trajectory history, *J. Geophys. Res.*, 101 (D19), 23 957–23 972, 1996.
- Hov, O., Stordal, F., and Eliassen, A.: Photochemical oxidant control strategies in Europe: A 19 days case study using a lagrangian model with chemistry, NILU TR5/95, 1985.
- Jacob, D. J., et al.: Origin of ozone and NO_x in the tropical troposphere: a photochemical analysis of aircraft observations over the southern Atlantic Basin, *J. Geophys. Res.*, 101 (D19), 24 235–24 250, 1996.
- Jonson, J. E. and Isaksen, I. S. A.: Tropospheric ozone chemistry. The impact of cloud chemistry, *J. Atmos. Chem.*, 16, 99–122, 1993.
- Lattuati, M.: Impact des émissions européennes sur le bilan de l'ozone troposphérique à l'interface de l'Europe et de l'Atlantique Nord: apport de la modélisation lagrangienne et des mesures en altitude, Ph. D. thesis, Univ. of Paris VI, 1997.
- Middleton, P., Stockwell, W. R., and Carter, W. P. L.: Aggregation and analysis of volatile organic compounds emissions for regional modelling, *Atmos. Environ.*, 24a (5), 1107–1133, 1990.
- Randriambelo, T., Baldy, S., Bessafi, M., and Despinoy, M.: An improved detection and characterization of active fires and smoke plumes in southeastern Africa and Madagascar, *Int. J. Rem. Sens.*, 19 (14), 2623–2638, 1998.
- Randriambelo, T., Baray, J.-L., and Baldy, S.: Effect of biomass burning, convective venting, and transport on tropospheric ozone over the Indian Ocean: Reunion Island field observations, *J. Geophys. Res.*, 105 (D9), 11 813–11 832, 2000.
- Sandholm, S., et al.: Summertime partitioning and budget of NO_y compounds in the troposphere over Alaska and Canada: ABLE 3B, *J. Geophys. Res.*, 99, 16 841, 1837–1861, 1994.
- Simpson, D.: Long period modeling of photochemical oxidants in Europe. Model calculations for July 1985, *Atmos. Environ.*, 25, 1609–1634, 1992.
- Smyth, S. B., et al.: Factors influencing the upper tropospheric distribution of reactive nitrogen over South Atlantic during the TRACE-A experiment, *J. Geophys. Res.*, 101 (D19), 24 165–24 186, 1996.
- Taupin, F. G.: Analyse et modélisation de la variabilité de l'ozone troposphérique en zone tropicale – Influence du brûlage de biomasse, Ph. D. thesis, Univ. of Clermont-Ferrand, 1998.
- Taupin F. G., Bessafi, M., Baldy, S., and Bremaud, P. J.: Tropospheric ozone above southwestern Indian ocean is strongly linked to dynamical conditions prevailing in the tropics, *J. Geophys. Res.*, 104 (D7), 8057–8066, 1999.
- Thompson, A. M., Pickering, K. E., McNamara, D. P., Schoeberl, M. R., Hudson, R. D., Kim, J. H., Browell, E. V., Kirchoff, V. W. J. H., and Nganga, D.: Where did tropospheric ozone over southern Africa come from in October 1992? Insights from TOMS, GTE TRACE A and SAFARI 1992. *J. Geophys. Res.*, 101 (D19), 24 251–24 278, 1996.